JOURNAL OF GEOPHYSICAL RESEARCH, VOL. 108, NO. A2, 1063, doi:10.1029/2002JA009548, 2003

Plasma instabilities in meteor trails: Linear theory

Meers M. Oppenheim, Lars P. Dyrud, and Licia Ray
Center for Space Physics, Boston University, Boston, Massachusetts, USA

Received 19 June 2002; revised 28 August 2002; accepted 4 September 2002; published 6 February 2003.

[1] Ablation of micrometeoroids between 70 and 130 km altitude in the atmosphere creates plasma columns with densities exceeding the ambient ionospheric electron density by many orders of magnitude. Density gradients at the edges of these trails can create ambipolar electric fields with amplitudes in excess of 100 mV/m. These fields combine with diamagnetic drifts to drive electrons at speeds exceeding 2 km/s. The fields and gradients also initiate Farley-Buneman and gradient-drift instabilities. These create field-aligned plasma density irregularities which evolve into turbulent structures detectable by radars with a large power-aperture product, such as those found at Jicamarca, Arecibo, and Kwajalein. This paper presents a theory of meteor trail instabilities using both fluid and kinetic methods. In particular, it discusses the origin of the driving electric field, the resulting electron drifts, and the linear plasma instabilities of meteor trails. It shows that though the ambipolar electric field changes amplitude and even direction as a function of altitude, the electrons always drift in the positive $\nabla n \times \mathbf{B}$ direction, where n is the density and B the geomagnetic field. The linear stability analysis predicts that instabilities develop within a limited range of altitudes with the following observational consequences: (1) nonspecular meteor trail echoes will be field-aligned; (2) nonspecular echoes will return from a limited range of altitudes compared with the range over which the head echo reflection indicates the presence of plasma columns; and (3) anomalous cross-field diffusion will occur only within this limited altitude range with consequences for calculating diffusion rates and temperatures with both specular and nonspecular radars. *INDEX TERMS:* 6245 Planetology: Solar System Objects: Meteors; 2439 Ionosphere: Ionospheric irregularities; 2435 Ionosphere: Ionospheric disturbances; 2471 Ionosphere: Plasma waves and instabilities; *KEYWORDS:* meteor, trail, radar, plasma, instability, turbulence

Citation: Oppenheim, M. M., L. P. Dyrud, and L. Ray, Plasma instabilities in meteor trails: Linear theory, *J. Geophys. Res.*, *108*(A2), 1063, doi:10.1029/2002JA009548, 2003.

1. Introduction

[2] Radars probing the atmosphere between 70 km and 130 km frequently receive echoes from plasma trails left by ablating meteoroids. These echoes have proven useful in determining the speeds, directions of origin, and, to a lesser extent, the masses of small meteoroids. Meteor trail echoes are also used extensively to estimate mesospheric and thermospheric temperatures and wind velocities. However, meteor plasmas contain large amounts of free energy which can drive rapid plasma drifts and instabilities. This paper develops the plasma physics of meteor trails and applies this theory to explain the origin and characteristics of radar measurements. A companion paper in this same issue, entitled "Plasma instabilities in meteor trails: 2-D simulation studies" by *Oppenheim et al.* [2003] describes kinetic particle-in-cell simulations of meteor trails with characteristics analogous to those analyzed in this paper.

[3] *Chapin and Kudeki* [1994a] suggested that long-duration, nonspecular radar echoes of meteor trails observed at the geomagnetic equator result from a Farley-Buneman instability mechanism [see also, *Chang et al.*,1999]. *Oppenheim et al.* [2000] used kinetic plasma simulations to show that meteor trails can easily develop a Farley-Buneman/Gradient Drift (FBGD) type instability driven by a combination of the meteor trail's self-generated ambipolar electric field and the polarization electric field common in the E-region ionosphere. This instability creates field-aligned irregularities which rapidly develop into plasma turbulence easily detected by large radars. *Dyrud et al.* [2001] subsequently showed that FBGD waves develop without an external electric field and also demonstrated that the waves and turbulence cause an anomalous diffusion much larger than the expected cross-field ambipolar diffusion. In this paper, we develop the linear plasma theory of meteor trails. Further, we predict the altitude range at which one expects to find field-aligned irregularities (FAI) and therefore nonspecular meteor trails.

[4] This paper is organized as follows. First, we review the motivating observations for this work and the previous theoretical studies of meteor trails and related topics. Second, we describe the two-fluid, steady-state solution for meteor trail diffusion and point out a number of new

0148-0227/03/2002JA009548

and important features of this solution. Third, using this solution as a starting point, we evaluate the stability of a two-fluid meteor trail and show conditions for instability. Fourth, we extend this analysis by evaluating stability while assuming that kinetic effects modify ion dynamics. This is applied to the stability of meteor trails as a function of altitude. Finally, our conclusion summarizes our findings.

2. Background

[5] Meteors create three principal types of returns detectable by radars. The first and most common radar detection occurs when an ablating meteoroid creates a trail lying perpendicular to a radar's beam. These specular meteor trails were originally detected in the 1930s and 1940s when radars were first pointed at the ionosphere. Today, many hundreds of radars have been built to explicitly detect specular echoes and use the information to study atmospheric winds and temperatures and to characterize the solar system's micrometeoroids [*Ceplecha et al.*, 1998].

[6] The second type of echoes detected by radars are short duration returns (typically a few pulse periods) which are extended in range. These ''head echoes'' appear to follow the meteoroid as it travels through the atmosphere. This type of echo was first observed in the late 1940s because they can only be detected by radars with a large aperture-power product [*McKinley and Millman*, 1949]. The ALTAIR, Arecibo, Jicamarca, EISCAT and MU radars all frequently observe head echoes [*Close et al.*, 2000; *Janches et al.*, 2000; *Chapin and Kudeki*, 1994b; *Pellinen-Wannberg et al.*, 1998; *Mathews et al.*, 1997]. A full understanding of the radar and plasma physics of head echoes remains an area of ongoing research [*Zhou et al.*, 1998; *Wannberg et al.*, 1996; *Close et al.*, 2002].

[7] Radars occasionally observe a third type of meteor echo, returns from meteor trails not aligned perpendicular to the radar beam. These ''nonspecular'' meteor trails have been observed since the early 1960s and were initially thought to result from roughness in the trail ionization distribution or wind shears [*McKinley*, 1961]. Over 30 years later, *Chapin and Kudeki* [1994a] presented observations of nonspecular trails and interpreted their origin as plasma instabilities, in particular the Farley-Buneman instability driven by the presence of the electrojet **E**-field. In the last few years, many papers have reported observations of nonspecular meteor trails from a range of locations. *Haldoupis and Schlegel* [1993] and *Zhou et al.* [2001] have reported meteor trail measurements at midlatitudes. *Reddi and Nair* [1998] presented measurements at low latitudes but outside the electrojet. These echoes typically last for less than 1 second but can persist for as long as a few minutes. *Chapin and Kudeki* [1994a] speculated that the long-lived trails remain unstable for so long because they trigger instabilities in a nearly unstable electrojet.

[8] The fundamental behavior of meteor trails and collisionally dominated plasmas has been discussed in many books and review articles [*Öpik*, 1958; *Ceplecha et al.*, 1998; *Rishbeth and Garriott*, 1969]. More specifically, a number of authors have evaluated the ambipolar diffusion of meteor trails in collisional plasmas [*Pickering and Windle*, 1970; *Jones*, 1991; *Robson*, 2001]. Most of our understanding of weakly ionized meteor trails derives from radar observations and relies on detailed analyses of the precise interaction between meteor trails and radar signals [*Jones and Jones*, 1991]. Other researchers have investigated similar electrodynamics generated by barium cloud releases [*Blaunstein et al.*, 1993].

[9] The linear theory describing meteor trail instabilities resembles the linear theory of the two principle *E* region instabilities, the Farley-Buneman and the gradient-drift instabilities [*Farley*, 1963; *Buneman*, 1963; *Maeda et al.*, 1963]. Numerous papers and a few books discuss the fluid theory of these instabilities [*Farley*, 1985; *Fejer et al.*, 1984; *Kelley*, 1989]. Several papers address the kinetic plasma physics necessary to describe short wavelength modes [*Schmidt and Gary*, 1973; *Lee et al.*, 1971]. Recently, theoretical studies of thermal corrections of the Farley-Buneman instability have shown the complexity of this instability [*Dimant and Sudan*, 1995; *Kissack et al.*, 1997; *Dimant and Sudan*, 1997; *Kagan and Kelley*, 2000]. While our current research neglects this aspect of the instability, thermal effects may prove relevant in meteor instabilities as well.

3. Theory of Meteor Trail Plasmas

[10] A micrometeoroid ($\lesssim 10^{-5}$ kg) ablating in the upper atmosphere creates a narrow column of energetic neutrals and plasma. This column expands rapidly until slowed and cooled by collisions. The radius of the column at the point when it transitions from a rapid kinetic expansion to a slower diffusive expansion, called the initial radius of the trail, is somewhat smaller than the mean free path length [*Baggaley*, 1981; *Bronshten*, 1983]. After the column reaches this initial radius, the dynamics of the expanding column of charged particles may be approximately described as a plasma fluid.

[11] Above 75 km in altitude and perpendicular to the geomagnetic field, **B**, electrons are highly magnetized while ions are de-magnetized by collisions. As the trail plasma expands beyond its initial radius, a strong ambipolar electric field develops as a result of the differing ion and electron mobilities. The electrons respond to this cross-field ambipolar field by $\mathbf{E} \times \mathbf{B}$-drifting perpendicular to both **B** and the density gradient of the meteor trail. This drift, combined with the plasma density gradients, can generate an unstable plasma [*Fejer et al.*, 1975]. This instability leads to the formation of waves which rapidly develop into turbulence. This field-aligned instability also creates plasma density perturbations visible to radars, allowing for nonspecular radar reflections [*Oppenheim et al.*, 2000]. Further, it causes anomalous diffusion, affecting the meteor trail's expansion rate [*Dyrud et al.*, 2001]. The following sections describe how the electric fields, electron drifts, and instabilities depend upon the altitude and trail density.

3.1. Equilibrium Condition

[12] In order to evaluate the stability of a meteor trail, we must first define an equilibrium state. We will use the cross-field ambipolar expansion of a diffusing plasma column perpendicular to the magnetic field, **B**. We conduct this analysis only in the plane perpendicular to **B**, and assume that in the plane parallel to **B** the trail expands through unmagnetized ambipolar diffusion and is not unstable to

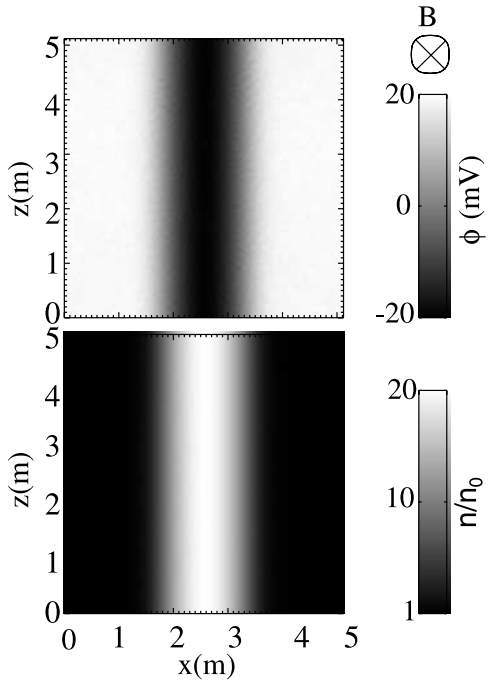

Figure 1. Electric potential, ϕ, in volts (top) and plasma density enhancements, n_e/n_0, (bottom) for a slab trail perpendicular **B**. The magnitude of each quantity is represented by the grey-scale bar to the right.

plasma instabilities [*Kudeki and Farley*, 1989]. For this equilibrium state, we will assume the ions are an isothermal, collisional, and unmagnetized fluid plasma such that

$$\mathbf{v}_i = -\mu_i \nabla\phi - D_i \nabla s, \qquad \mu_{i,e} \equiv \frac{e}{m_{i,e}\nu_{i,e}} \quad \text{and} \quad D_{i,e} \equiv \frac{K_B T_{i,e}}{m_{i,e}\nu_{i,e}} \tag{1}$$

where $\mu_{i,e}$ defines the ion and electron mobilities, $D_{i,e}$ defines the ion and electron diffusion rates, $\nu_{i,e}$ is the collision rate for the ions or electrons with the background neutral gas (mostly N_2), ϕ is the electric potential, and $\nabla s \equiv \nabla n/n = \nabla \ln (n/n_b)$ defines the gradient of the log of the plasma density normalized to the background plasma density, n_b. The electrons are an inertialess and magnetized fluid whose velocity perpendicular to **B** can be expressed as

$$\mathbf{v}_{e\perp} = \mu_{e\perp}\nabla\phi - D_{e\perp}\nabla s + \frac{\mathbf{v}_{E\times B} + \mathbf{v}_D}{1 + \nu_e^2/\Omega_e^2} \tag{2}$$

where

$$\mu_{e\perp} \equiv \frac{\mu_e}{1+\Omega_e^2/\nu_e^2}, \quad D_{e\perp} \equiv \frac{D_e}{1+\Omega_e^2/\nu_e^2},$$
$$\mathbf{v}_{E\times B} \equiv \frac{E\times B}{B^2}, \quad \mathbf{v}_D \equiv -\frac{k_B T_e}{e}\frac{\nabla s \times B}{B^2},$$

where $\mathbf{v}_D$ is the diamagnetic drift, and $\Omega_e = e\vec{B}/m_e$ is the electron cyclotron frequency (see *Chen* [1984, p. 171], for an explanation of these terms). For altitudes above 85 km, $\Omega_e^2/\nu_e^2 \gg 1$ and electrons predominantly engage in $\mathbf{E} \times \mathbf{B}$ and diamagnetic drifts, as described by the third term of equation (2).

[13] The assumption of quasi-neutrality, $\nabla \cdot \mathbf{J} = 0$, where J is the current, allows us to combine (1) and (2) to generate an expression for the electric potential ($\perp$ to **B**) in terms of density,

$$\mu_T \nabla\cdot(n\nabla\phi) - D_T\nabla^2 n - \frac{\nabla n\cdot\nabla\phi\times\mathbf{B}_0}{B_0^2\left(1+\Omega_e^2/\nu_e^2\right)} = 0, \qquad D_T \equiv D_{e\perp} - D_i T \equiv \mu_{e\perp} + \mu_i. \tag{3}$$

This equation allows us to solve for the cross-field ambipolar electric potential, ϕ, for a prescribed density distribution, n, and visa-versa.

[14] For many simple trail geometries one can easily solve equation (3) analytically. For example, in Cartesian coordinates we can align the magnetic field, **B**, along the $\hat{y}$ direction and assume homogeneity along both $\hat{y}$ and $\hat{z}$. This allows the density gradient to vary only along $\hat{x}$. Figure 1 shows a trail with this geometry. While homogeneity along **B** is unrealistic, at high altitudes one expects trails stretched in the direction parallel to **B**, so this assumption is not entirely implausible. An alternate geometry which may be evaluated in cylindrical coordinates aligns the trail parallel to **B**, leaving a circular cross-section perpendicular to **B**. As long as ∇n is perpendicular to $\mathbf{E} \times \mathbf{B}$, equation (3) becomes simply,

$$\nabla\cdot(n\nabla\phi) = D_T/\mu_T\nabla^2 n \tag{4}$$

and may be easily solved for either slab or cylindrical geometries.

[15] In the case of a slab trail as shown in Figure 1,

$$E_x = -\frac{D_T}{\mu_T}\frac{\partial s}{\partial x} + \frac{C}{n} \tag{5}$$

where C is a constant of integration set by boundary conditions. If we further assume that the density of the trail is the sum of a Maxwellian plus a background density, $n = n_0 \exp(-x^2/x_0^2) + n_b$, then equation 5 gives the ambipolar field

$$E_x = -\frac{D_T}{\mu_T}\left[\frac{n_0 \exp\left(-x^2/x_0^2\right)\left(-2x/x_0^2\right)}{n_0 \exp\left(-x^2/x_0^2\right) + n_b}\right]. \tag{6}$$

[16] Figure 1 shows the ambipolar electric field for a trail at 102 km at 8 am local time with a Maxwellian density profile and other parameters specified in Table 1. Due to the limitation of grey-scale figures we have chosen to plot the electric potential, ϕ. A trail, perfectly aligned along **B**, develops the same electric field except $x \rightarrow r$. A trail making a 45° angle with respect to **B** will have an oval cross-section and will develop similar fields and potentials.

[17] For the system shown in Figure 1, the ion cross-field mobility, $\mu_i \sim \mu_{i\perp}$ exceeds the electron one, $\mu_{e\perp}$. In

Table 1. Physical Parameters for 102 km Equatorial Ionosphere

Parameter	Value
External magnetic field, B_0	2.9×10^{-5} T
Neutral gas density, n_n	7.1×10^{18} m^{-3}
Temperature, $T_{i,n}$	250 K
e^--neutral collision frequency, ν_{en}	3.0×10^4 s^{-1}
Ion mass, m_i	5.0×10^{-26} kg
Peak/background ratio, n_e/n_0	30
Trail line density, N_{line}	2.7×10^{13} m^{-1}
Background e^- density, n_0	1.1×10^{11} m^{-3}
Trail radius, r_t	1.5 m
Ion-neutral collision frequency, ν_{in}	2.8×10^3 s^{-1}

this case, the electric field points toward the center of the trail and prevents the ions from escaping from the magnetized and less mobile electrons. At different altitudes, the changing collision rates alter the relationship between these mobilities. Below ~100 km (near the magnetic equator), the collision rates become high enough that the electron diffusion rate exceeds the ion rate causing the ambipolar electric field to reverse directions.

[18] The transition altitude where **E** shifts from pointing inward toward the trail center to outwards depends on latitude because of the changing geomagnetic field.

3.2. Equilibrium Electron Drifts

[19] Electron drift motion results from the combination of **E** × **B** and diamagnetic drifts where, in the absence of external electric fields or, equivalently, neutral winds, E arises from the self-generated ambipolar electric fields. Combining equations (2) and (4) makes the electron drift velocity

$$\mathbf{v}_{e\perp} = \left(\frac{D_T}{\mu_T} + \frac{D_e}{\mu_e}\right)\frac{\nabla s \times \hat{B}}{|B|} - \left(D_{e\perp} - \mu_{e\perp}\frac{D_T}{\mu_T}\right)\nabla s \qquad (7)$$

where $\hat{B} \equiv \mathbf{B}/|B|$. In the case where electron motion lies purely perpendicular to ∇n, this simplifies to

$$\mathbf{v}_{e\perp} = \frac{C_s^2}{\Omega_i(1+\Psi_0)}\nabla s \times \hat{B}, \qquad C_s^2 \equiv \sqrt{\frac{k_B(T_e+T_i)}{m_i}} \text{ and } \Psi_0 \equiv \frac{\nu_e\nu_i}{\Omega_e\Omega_i} \qquad (8)$$

where C_s is the ion acoustic velocity and Ψ_0 is a ratio that shows up repeatedly in E region dynamics. This equation tells us that, regardless of the direction of **E**, the electrons always drift in the positive $\nabla n \times \hat{B}$ direction. At high altitudes **E** × **B** drifting dominates, but at lower altitudes, as **E** changes sign, the electrons continue to drift in the same direction. This occurs because the diamagnetic drift rate, $\mathbf{v}_D$, becomes larger, preventing the electrons from reversing direction. Figure 2 compares drift velocities as a function of altitude for a trail with $\nabla s = 1$ m^{-1}. Electron velocity scales linearly with ∇s and Figure 1 shows a trail with $\nabla s = 4$ m^{-1} at 102 km altitude which results in drifts of ~5.2 km/s. These drifts combined with the density gradients drive the instabilities discussed in *Dyrud et al.* [2001] and *Oppenheim et al.* [2000].

[20] A single fluid (MHD-like) approach gives us a better understanding of why the electrons always rotate in the positive $\nabla n \times \mathbf{B}$ direction. Simply,

$$\mathbf{J}\times\mathbf{B} + \mathbf{R}_n = \nabla p,$$

where p is the pressure, J is the current, and

$$\mathbf{R}_n \equiv -m_i n_i \nu_i \mathbf{v}_i - m_e n_e \nu_e \mathbf{v}_e$$

is the collision with neutrals (friction) term, necessary within the ionosphere. Since the pressure drives all meteor trail evolution, the combination of **J** × **B** and $\mathbf{R}_n$ must combine to equal ∇p and the radial component must always have the same sign as at ∇p. At high altitudes, collisions with neutrals are rare and, hence, R_n is small. This means that the radial component of **J**, can be calculated by **J** × **B** = ∇p. As one descends to lower altitudes, **R** increases and **J** × **B** decreases until eventually **R** ≈ ∇p. At no point can **R** ever exceed ∇P and cause **J** to reverse directions.

[21] We can generate an equation for cross-field ambipolar diffusion using equation (8) and the continuity equation for the case where the symmetry eliminates the cross-field terms in equations (8) and (3):

$$\frac{\partial n}{\partial t} = D_{a\perp}\nabla^2 n, \; Da_\perp \equiv \left(D_{e\perp} - \mu_{e\perp}\frac{D_T}{\mu_T}\right). \qquad (9)$$

The resulting diffusion coefficient, $D_{a\perp}$, typically predicts slow trail expansion perpendicular to **B**. However, this diffusion rate neglects dynamics parallel to **B** and perturbations along the trail, both of which will often play a dominant role. One of the purposes in describing the instabilities and waves in this paper and in the companion paper is to show how an E region plasma column will spontaneously develop density perturbations which will

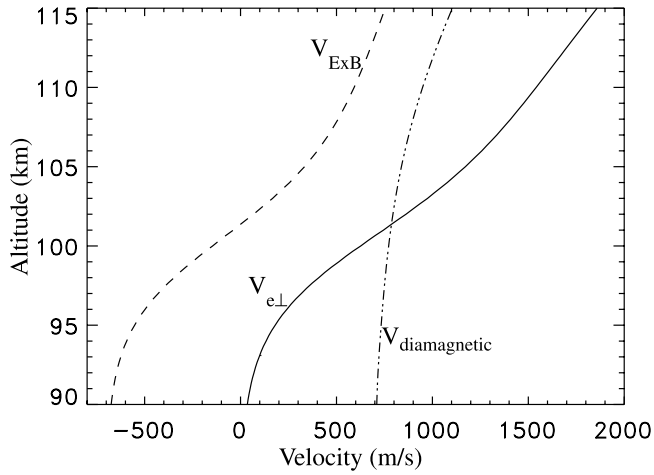

Figure 2. Electron velocity vs. altitude assuming parameters from the international reference ionosphere (IRI) for the geomagnetic equator at 8 am L.T. and $\nabla n/n = 1$ m^{-1}. $V_{\mathbf{E}\times\mathbf{B}}$ shows the **E** × **B** drift velocity; $V_{\nabla n\times\mathbf{B}}$ shows the diamagnetic drift velocity; and $V_{e\perp}$ shows the sum of the two velocities.

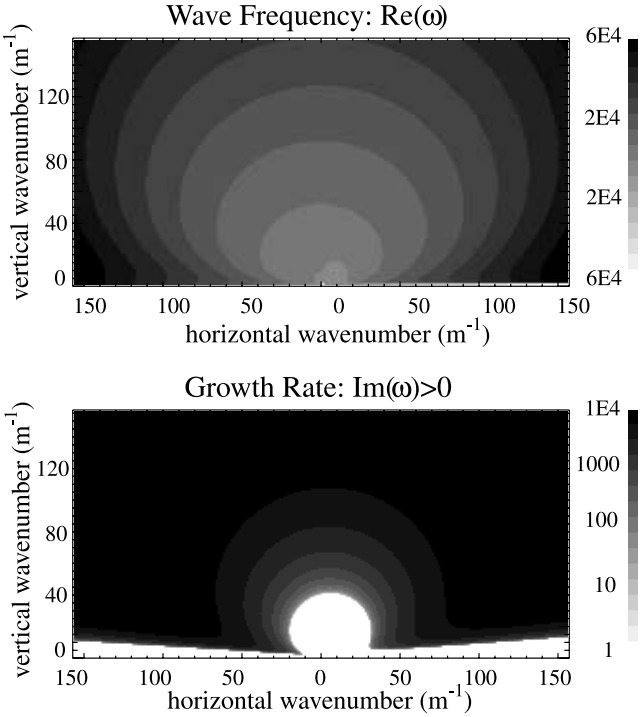

Figure 3. Shows the real (top) and imaginary (bottom) parts of ω as a function of vertical and horizontal wavenumber, $\mathbf{k}$. Of the two roots, only the one with the larger ω_i is shown. The bottom panel only shows values for $\omega_i > 0$.

dramatically increase the diffusion rate beyond that described by equation (9).

3.3. Stability

[22] Linear plasma theory allows us to evaluate the stability of these meteor trails. Further, it gives us insight into the phase and group velocities and growth or damping of any wave which might develop within the trail. Since radars are extremely sensitive to plasma waves, understanding the characteristics of these waves should allow us to better understand nonspecular radar echoes.

3.3.1. Fluid Stability

[23] Assuming both the electrons and ions behave as plasma fluids, we can recreate the FBGD dispersion relation described in *Fejer et al.* [1984]. To obtain the dispersion relation, we assume inertialess electrons as in equation (2) and quasi-neutrality as before, but keep ion inertia. The linear, Fourier transformed, ion momentum equation remains the same as equation (1) except $\nu_i \rightarrow \nu_i - i\omega$ where ω is the complex wave frequency. With these assumptions the following relation may be derived:

$$\omega - \mathbf{k}\cdot\mathbf{v}_{e0} = -A\left[(\omega - \mathbf{k}\cdot\mathbf{v}_{i0})(\nu_i - i\omega) + ik^{\dagger 2}C_s^2\right]$$
$$A \equiv \left(\frac{\Psi_0}{\nu_i} - \frac{i}{\Omega_i}\frac{\mathbf{k}\cdot\nabla s_0\times\hat{B}}{k^{\dagger 2}}\right) \tag{10}$$

where $\mathbf{v}_{i0}$ and $\mathbf{v}_{e0}$ are the equilibrium (drift) velocities of each species; $\nabla s_0 \equiv \nabla n_0/n_0$ is the initial density gradient scale length; $k^{\dagger 2} \equiv (\mathbf{k} - i\nabla s_0)\cdot\mathbf{k}$.

[24] When applying this equation to E-region gradient drift and Farley-Buneman instabilities, one typically assumes that $\nu_i \gg \omega_r \gg \omega_i$ where $\omega \equiv \omega_r + i\omega_i$. These assumptions allow one to simplify equation (10) to

$$\omega_r = \mathbf{k}\cdot\mathbf{v}_{e0}/(1+\Psi_0) \qquad \text{(incorrect)}$$
$$\omega_i = \frac{\Psi_0/\nu_i}{1+\Psi_0}\left(w_r^2 - k^2C_s^2 + \frac{\omega_r\mathbf{k}\cdot\nabla s_0\times\hat{z}}{\Psi_0\Omega_i k^2}\right) \tag{11}$$

which do not apply to meteor trails. In the case of meteor trails, ω_r often has a similar magnitude as ω_i and ν_i and, therefore, one must solve equation (10) as a quadratic equation.

[25] Two assumptions do apply, allowing some simplification of equation (10). If $\mathbf{B} = \mathbf{B}_0\hat{z}$, then A simplifies to

$$A \equiv \Psi_0/\nu_i - (i/\Omega_i)\mathbf{k}\cdot\nabla s_0\times\hat{z}/k^{\dagger 2}, \tag{12}$$

and if $\mathbf{v}_{i0}$ is negligible compared to $\mathbf{v}_{e0}$, which it always is for E region plasmas, the quadratic equation simplifies to

$$\omega - \mathbf{k}\cdot\mathbf{v}_{e0} = -A\left[\left(\nu_i\omega - i\omega^2\right) + ik^{\dagger 2}C_s^2\right]. \tag{13}$$

[26] A few interesting points about applying the dispersion relation, equation 10, to meteor trails follow. First, in Farley-Buneman theory, the $\mathbf{k}\cdot\mathbf{v}_{e0}$ term drives the instability. For meteor trails, with no driving external electric field, the $Aik^{\dagger 2}C_s^2$ term also contains a real component which always exceeds the $\mathbf{k}\cdot\mathbf{v}_{e0}$ term such that adding the real components of the two terms yields

$$\Re\left[Aik^2C_s^2 - \mathbf{k}\cdot\mathbf{v}_{e0}\right] = \frac{C_s^2k\cdot\nabla s_0\times\hat{B}}{\Omega_i}\frac{\Psi_0}{1+\Psi_0}. \tag{14}$$

This assumes that $\nabla s_0 \cdot k/k^2 \ll 1$, which applies when $\mathbf{k}$ represents waves aligned mostly perpendicular to the gra-

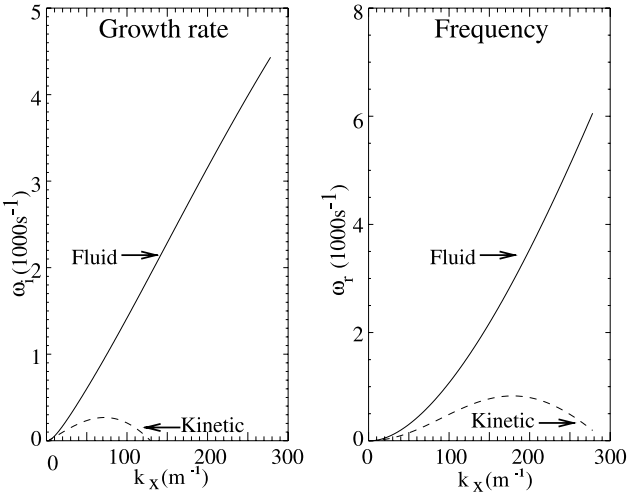

Figure 4. The left plot shows growth rate, ω_i, versus wavenumber, k_x, from fluid (solid line) and kinetic (dashed line) dispersion relations. The right figure shows the frequencies, ω_r. Calculations were done for the ionosphere at 102 km as shown in Table 1.

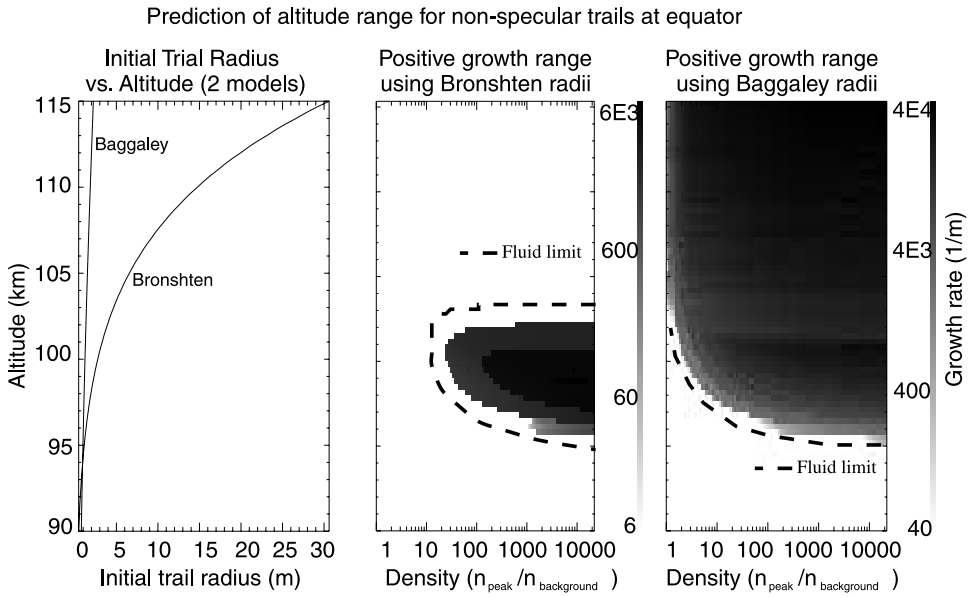

Figure 5. Left panel plots initial radius of trail versus altitude for the Baggaley and Bronshten models for a meteor traveling 60 km/s. The center panel shows the predicted growth rate as a function of altitude and peak plasma density, n_0/n_b, for the radius suggested by the Bronshten model. The right panel shows the same for the radius suggested by the Baggaley model. The dashed lines show the boundary between growing and damped instabilities calculated using the fluid instability equation assuming the smallest permissible wavelength is twice the Debye length.

dient, ∇s. Second, while the diamagnetic term dominates the electron drift velocity, diamagnetic drifts are divergence free and, therefore, do not contribute to driving the instability.

[27] Figure 3 shows an example of a solution to equation (13) for the parameters shown in Table 1. Particle-in-cell simulations, described and discussed in the companion paper, demonstrate that waves grow for a system with these parameters. Though Figure 3 shows increasing growth rates for increasing values of $|k|$, the simulation shows a peak wavelength at ~20 cm. While fluid equations accurately represent the physics at the longest unstable wavelengths and the conditions for instabilities, one needs a kinetic theory to predict which wavelengths grow the fastest.

3.3.2. Kinetic Theory of Stability

[28] Fluid plasma theory ignores kinetic phenomena. In particular, at short wavelengths, we expect ion Landau damping to reduce the growth rate [*Schmidt and Gary*, 1973; *Lee et al.*, 1971]. (Note that a minor error exists in the *Schmidt and Gary* [1973] paper: The first term in the denominator of equation (3) should be multiplied by -1.) To derive a dispersion relation which incorporates this physics, we assume warm, inertial, magnetized and fluid electrons, fully kinetic but unmagnetized ions and use Poisson's equation. The resulting dispersion relation describing modes perpendicular to both ∇n and B is

$$\begin{aligned} 0 &= H_i - H_e + k_x \\ H_i &\equiv \frac{\omega_{pi}^2(1.0+\beta Z(\beta))}{-v_{ith}^2 k_x - i\nu_i v_{ith} Z(\beta)/\sqrt{2}} \\ H_e &\equiv \frac{\omega_{pe}^2 k_x\left(\nu_e/\Omega_e^2 - i/(L_n\Omega_e k_x)\right)}{-i\omega + ik_x v_d + k_x^2 v_{eth}^2\left(\nu_e/\Omega_e^2 - i/(L_n\Omega_e k_x)\right)} \\ \beta &\equiv (w+i\nu_i)/\left(\sqrt{2}v_{ith}k_x\right) \end{aligned} \tag{15}$$

where $L_n = (\nabla n/n)^{-1}$ is the gradient length scale, $\omega_{pi}^2 = ne^2/(\varepsilon_0 m_i)$ is the ion plasma frequency and $Z(\beta)$ is the plasma dispersion function [*Chen*, 1984].

[29] Figure 4 illustrates the importance of the kinetic effect by comparing solutions of the fluid and kinetic dispersion relations. The fluid solution shows growth for wavelengths even much shorter than a Debye length while the kinetic solution shows a distinct peak at a given wave number and limited range of unstable wavelengths. It also shows that the frequency and, therefore, the phase velocity changes from that predicted by the fluid dispersion relation. Note that if we calculate growth rates by assuming quasi-neutrality instead of using Poisson's equation in the deriva-

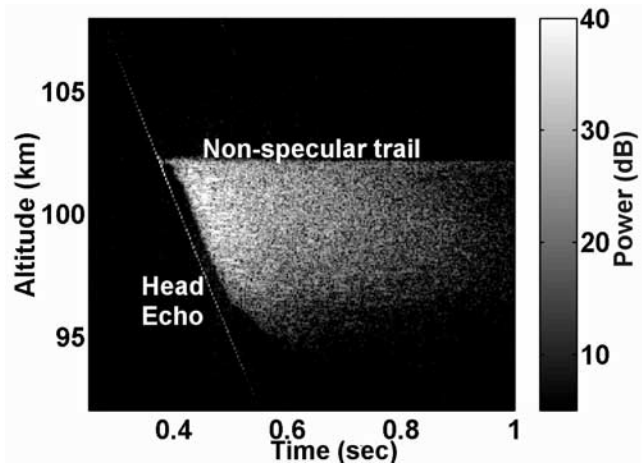

Figure 6. Example of a trail echo recorded by the VHF ALTAIR radar at the Kwajalein missile range as a function of altitude and time (Courtesy of *Close et al.* [2002]).

tion of the dispersion relation, then our results incorrectly predict a ~30% longer fastest growing wavelength.

[30] This analysis oversimplifies the physics of real meteor trails. It assumes a constant and essentially infinitely long gradient scale length, L_n. It also neglects any electron thermal or kinetic effects which could modify the solution further.

3.3.3. Criteria for Instability Onset

[31] Our analysis of meteor trail instabilities allows us to predict the range of altitudes where we expect field-aligned irregularities to develop. Figure 5 shows positive growth rates as a function of altitude and peak plasma density for meteor trails having a Maxwellian density profile, $n = n_0\exp(-r^2/r_0^2) + n_b$. To set the crucial scale length, r_0, we used two initial radius equations: the theoretical [*Bronshten*, 1983] prediction and the [*Baggaley*, 1981] equations which were based on underdense radar measurements. One can see that the instability growth rate depends strongly on the initial radius and only weakly on the peak plasma density. The minimum altitude is mostly determined by the high collision rates and depends only weakly on meteor parameters.

[32] A number of factors control the minimum altitude at which instabilities occur. First, at higher latitudes than the equatorial case shown in Figure 5, **B** increases causing the electron mobility to decrease. This causes the instability threshold to move down by as much as a few kilometers. Second, lighter ion species, such as O^+, have higher ion mobilities than the assumed Si^+ and will cause a drop in the minimum altitude.

[33] The initial radius of the trail determines ∇s which primarily controls the maximum instability altitude. The *Bronshten* [1983] values allow us to predict instability over a limited altitude range. The smaller radii predicted by *Baggaley* [1981] lead us to predict essentially no ceiling on the instability altitude. Nonspecular trail observations showing that the maximum nonspecular trail altitude matches that predicted using the *Bronshten* [1983] values for initial radius gives a new approach to resolving the long-standing problem of meteor trail initial radius [*Dyrud et al.*, 2002].

3.3.4. Observational Evidence for Onset Criteria

[34] The observational data shows nonspecular trails over a limited range of altitudes. Figure 6 shows a strong trail at high resolution. The line on the left hand side of the image results from the head echo [*Close et al.*, 2002]. The trail echo on the right spans a smaller range of altitudes than did the head echo. This difference occurs frequently and is discussed in more detail in *Dyrud et al.* [2002].

4. Conclusions

[35] Using both fluid and kinetic descriptions of meteor trail plasma dynamics, we have developed a local theory of instabilities which allows us to better explain simulations and observations of meteor trails by large power-aperture product radars and classical meteor radars. The comparison with simulations will be discussed further in the companion paper. We started by solving for the equilibrium state of a diffusing meteor trail perpendicular to **B** and showing that both the electron diamagnetic drift and $\mathbf{E} \times \mathbf{B}$ drift contribute to the total electron drift. We were able to demonstrate that the total electron drift always travels in the $\nabla n \times \mathbf{B}$ direction, even when the $\mathbf{E} \times \mathbf{B}$ drift drives electrons in the opposite direction. We then evaluated the linearized fluid system of equations around this equilibrium state, showing that the simplified forms of the FBGD assumptions of equation (11) do not apply to meteor trails and that one must solve the complete quadratic dispersion relation. We then described and solved the kinetic equations which show how ion Landau damping eliminates short wavelength modes. This will prove useful in predicting the dominant instability wavelength seen in the simulations.

[36] The linear theory of meteor trails allows us to predict the altitude range where instabilities will grow. Making a number of assumptions about the state of "typical" meteor trails, we demonstrated that one expects instabilities only within a limited range of altitudes, typically between 95 and 105 km. The minimum altitude depends principally on the meteor plasma composition and latitude of the trail. The maximum altitude depends primarily on the gradient scale length of the trail which results from the initial radius of the meteor trail. We used this dependency to show that the *Bronshten* [1983] description of initial radius matches observations better than the description put forth by [*Baggaley*, 1981].

[37] **Acknowledgments.** The authors would like to thank Yakov Dimant for useful discussions, Kelly McMillon for editing and producing many of the figures, and Stephen Hunt and Sigrid Close for discussions and analysis of ALTAIR data. This material is based upon work partially supported by the National Science Foundation under Grant No. ATM9986976 and NASA Grant No. NGT5-50288.

[38] Arthur Richmond thanks W. G. Elford and David Hysell for their assistance in evaluating this paper.

References

Baggaley, W. J., Single wavelength measurements fo the initial radii of radio meteor ionization columns, *Bull. Astron. Inst. Czech.*, *32*, 345–348, 1981.

Blaunstein, N. S., G. P. Milinevsky, V. A. Savchenko, and E. V. Mishin, Formation and development of striated structure during plasma cloud evolution in the Earth's ionosphere, *Planet. Space Sci.*, *41*, 453–460, 1993.

Bronshten, V. A., *Physics of Meteoric Phenomena*, chap. 100–105, D. Reidel, Norwell, Mass., 1983.

Buneman, O., Excitation of field aligned sound waves by electron streams, *Phys. Rev. Lett.*, *10*, 285, 1963.

Ceplecha, Z., J. Borovicka, W. G. Elford, D. O. Revelle, R. L. Hawkes, V. Porubcan, and M. Simek, Meteor phenomena and bodies, *Space Sci. Rev.*, *84*, 327–471, 1998.

Chang, J. L., S. K. Avery, and R. A. Vincent, New narrow-beam meteor radar results at Christmas Island: Implications for diurnal wind estimation, *Radio Sci.*, *34*, 179–197, 1999.

Chapin, E., and E. Kudeki, Plasma-wave excitation on meteor trails in the equatorial electrojet, *Geophys. Res. Lett.*, *21*, 2433–2436, 1994a.

Chapin, E., and E. Kudeki, Radar interferometric imaging studies of long duration meteor echo observed at Jicamarca, *J. Geophys. Res.*, *99*, 8937–8949, 1994b.

Chen, F. F., *Introduction to Plasma Physics and Controlled Fusion*, 2nd ed., Plenum, New York, 1984.

Close, S., S. M. Hunt, M. J. Minardi, and F. M. McKeen, Analysis of Perseid meteor head echo data collected using the Advanced Research Projects Agency Long-Range Tracking and Instrumentation Radar (ALTAIR), *Radio Sci.*, *35*, 1233–1240, 2000.

Close, S., M. M. Oppenheim, S. Hunt, and L. P. Dyrud, Scattering characteristics of high-resolution meteor head echoes detected at multiple frequencies, *J. Geophys. Res.*, *107*(A10), 1295, doi:10.1029/2002JA009253, 2002.

Dimant, Y. S., and R. N. Sudan, Kinetic theory of the Farley-Buneman instability in the *E* region of the ionosphere, *J. Geophys. Res.*, *100*, 14,605–14,624, 1995.

Dimant, Y. S., and R. N. Sudan, Physical nature of a new cross-field current-driven instability in the lower ionosphere, *J. Geophys. Res.*, *102*, 2551–2564, 1997.

Dyrud, L. P., M. M. Oppenheim, and A. F. von Endt, The anomalous diffusion of meteor trails, *Geophys. Res. Lett.*, *28*, 2775–2778, 2001.

Dyrud, L. P., M. M. Oppenheim, S. Close, and S. Hunt, Interpretation of non-specular radar meteor trails, *Geophys. Res. Lett.*, *29*(21), doi:10.1029/2002JA009548, 2002.

Farley, D. T., A plasma instability resulting in field-aligned irregularities in the ionosphere, *J. Geophys. Res.*, *68*, 6083, 1963.

Farley, D. T., Theory of equatorial electrojet plasma waves: New developments and current status, *J. Atmos. Terr. Phys.*, *47*, 729, 1985.

Fejer, B. G., D. T. Farley, B. B. Balsley, and R. F. Woodman, Vertical structure of the VHF backscattering region in the equatorial electrojet and the gradient drift instability, *J. Geophys. Res.*, *80*, 1313, 1975.

Fejer, B. G., J. Providakes, and D. T. Farley, Theory of plasma waves in the auroral E region, *J. Geophys. Res.*, *89*, 7487, 1984.

Haldoupis, C., and K. Schlegel, A 50-MHz radio Doppler experiment for midlatitude E region coherent backscatter studies: System description and first results, *Radio Sci.*, *28*, 959–978, 1993.

Janches, D., J. D. Mathews, D. D. Meisel, and Q.-H. Zhou, Micrometeor Observations Using the Arecibo 430 MHz Radar, *Icarus*, *145*, 53–63, 2000.

Jones, W., Theory of diffusion of meteor trains in the geomagnetic field, *Planet. Space Sci.*, *39*, 1283–1288, 1991.

Jones, J., and W. Jones, Oblique-scatter of radio waves from meteor trains: Full-wave calculations, *Planet. Space Sci.*, *39*, 1289–1296, 1991.

Kagan, L. M., and M. C. Kelley, A thermal mechanism for generation of small-scale irregularities in the ionospheric E region, *J. Geophys. Res.*, *105*, 5291–5302, 2000.

Kelley, M. C., *The Earth's Ionosphere*, Academic, San Diego, Calif., 1989.

Kissack, R. S., J.-P. St.-Maurice, and D. R. Moorcroft, The effect of electron-neutral energy exchange on the fluid Farley-Buneman instability threshold, *J. Geophys. Res.*, *102*, 24,091–24,116, 1997.

Kudeki, E., and D. T. Farley, Aspect sensitivity of equatorial electrojet irregularities and theoretical implications, *J. Geophys. Res.*, *94*, 426, 1989.

Lee, K., C. F. Kennel, and J. M. Kindel, High-frequency Hall current instability, *Radio Sci.*, *6*, 209, 1971.

Maeda, K., T. Tsuda, and H. Maeda, Theoretical interpretation of the equatorial sporadic E layers, *Phys. Rev. Lett.*, *11*, 406, 1963.

Mathews, J. D., D. D. Meisel, K. P. Hunter, V. S. Getman, and Q. Zhou, Very high resolution studies of micrometeors using the Arecibo 430 MHz radar, *Icarus*, *126*, 157–169, 1997.

McKinley, D. W. R., *Metoer Science and Engineering*, McGraw-Hill, New York, 1961.

McKinley, D. W. R., and P. M. Millman, A phenomenological theory of radar echoes from meteors, *Proc. IRE*, *37*, 364–375, 1949.

Öpik, E. J., *Physics of Meteor Flight in the Atmosphere*, Wiley-Interscience, New York, 1958.

Oppenheim, M. M., A. F. vom Endt, and L. P. Dyrud, Electrodynamics of meteor trail evolution in the equatorial E-region ionosphere, *Geophys. Res. Lett.*, *27*, 3173–3176, 2000.

Oppenheim, M. M., L. P. Dyrud, and A. F. vom Endt, Plasma instabilities in meteor trails: 2-D simulation studies, *J. Geophys. Res.*, *108*, doi:10.1029/2002JA009548, in press, 2003.

Pellinen-Wannberg, A., A. Westman, G. Wannberg, and K. Kaila, Meteor fluxes and visual magnitudes from EISCAT radar event rates: A comparison with cross-section based magnitude estimates and optical data, *Ann. Geophys.*, *16*, 1475, 1998.

Pickering, W. M., and D. W. Windle, The diffusion of meteor trains, *Planet. Space Sci.*, *18*, 1153–1161, 1970.

Reddi, C. R., and S. M. Nair, Meteor trail induced backscatter in MST radar echoes, *Geophys. Res. Lett.*, *25*, 473–476, 1998.

Rishbeth, H., and O. D. Garriott, *Introduction to Ionospheric Physics*, Academic, San Diego, Calif., 1969.

Robson, R. E., Dispersion of meteor trails in the geomagnetic field, *Phys. Rev. E*, *63*, 26,404, 2001.

Schmidt, M. J., and S. P. Gary, Density gradients and the Farley-Buneman instability, *J. Geophys. Res.*, *78*, 8261, 1973.

Wannberg, G., A. Pellinen-Wannberg, and A. Westman, An ambiguity-function-based method for analysis of Doppler decompressed radar signals applied to EISCAT measurements of oblique UHF-VHF meteor echoes, *Radio Sci.*, *31*, 497–518, 1996.

Zhou, Q.-H., P. Perillat, J. Cho, and J. Mathews, Simultaneous meteor echo observations by large aperture VHF and UHF radars, *Radio Sci.*, *33*, 1641–1654, 1998.

Zhou, Q.-H., J. D. Mathews, and T. Nakamura, Implications of meteor observations by the MU radar, *Geophys. Res. Lett.*, *28*, 1299–1402, 2001.

L. P. Dyrud, M. M. Oppenheim, and L. Ray, Center for Space Physics, Boston University, 725 Commonwealth Ave, Boston, MA 02215, USA. (meerso@bu.edu)